# Photoelectron spectroscopy and density functional theory study of ConO− (n = 1−3)
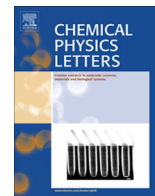
**5 AUTHORS**, INCLUDING:

Hong-Guang Xu

Chinese Academy of Sciences

**55** PUBLICATIONS **325** CITATIONS

# Photoelectron spectroscopy and density functional theory study of Co$_n$O$^-$ ($n$ = 1–3)

Ren-Zhong Li [a,b], Jun Liang [c], Xi-Ling Xu [b], Hong-Guang Xu [b], Wei-Jun Zheng [b,*]

[a] College of Electronics and Information, Xi'an Polytechnic University, Xi'an 710048, China
[b] Beijing National Laboratory for Molecular Sciences, State Key Laboratory of Molecular Reaction Dynamics, Institute of Chemistry, Chinese Academy of Sciences, Beijing 100190, China
[c] College of Physics and Electronic Information, Anhui Normal University, Wuhu 241000, China

## ABSTRACT

Co$_n$O$^-$ ($n$ = 1–3) clusters were investigated with photoelectron spectroscopy and density functional calculations. The vertical detachment energies (VDEs) of Co$_n$O$^-$ ($n$ = 1–3) were measured to be 1.54 ± 0.04, 1.43 ± 0.08, and 1.42 ± 0.08 eV respectively from their photoelectron spectra. The electron affinity and term energy of CoO were determined to be 1.54 ± 0.04 eV and 0.31 ± 0.04 eV respectively based on the vibrationally resolved photoelectron spectrum of CoO$^-$ and theoretical calculations. The structures of Co$_n$O$^-$ ($n$ = 1–3) were determined by comparison of photoelectron experiments and calculations. The analysis of molecular orbitals shows that the HOMOs of Co$_n$O$^-$ ($n$ = 1–3) cluster anions are mainly localized on the Co atoms.

© 2013 Elsevier B.V. All rights reserved.

## 1. Introduction

In recent years, there is an increasing interest in cobalt-containing compounds and materials because of their novel electronic, magnetic and chemical properties. Cobalt oxides can be used as the electrode materials [1,2] and have been identified as an active catalyst for reduction of CO and NO$_x$ pollutants in the air [3–8]. A number of experimental and theoretical works have been performed on cobalt oxide clusters [9–26]. The flow tube experiment conducted by Kapiloff and Ervin showed that the reactivity of small Co$_n^-$ clusters ($n$ = 2–8) with O$_2$ is very high [16]. The reactions of neutral cobalt oxide clusters Co$_m$O$_n$ with CO, NO and C$_2$H$_2$ were investigated by Xie and co-workers [26] and they observed strong cluster size dependent behavior for all the oxidation reactions. Yin et al. [27] studied the formation and mass distribution of cationic cobalt oxide clusters and found that Co$_{11}$O$_{12}^+$ and Co$_{12}$O$_{12}^+$ clusters have a relatively high stability. The photodissociation mass spectra of Co$_x$O$_y^+$ by Dibble et al. [28] showed prominent stoichiometries of $x = y$. The density functional calculations suggested that CoO$_4$ has a diperoxide Co(O$_2$)$_2$ structure [29] and CoO$_2$ has a Co-dioxide structure [30]. For cobalt monoxide, there are some discrepancies on the electronic transition energy and the anion electronic state in the literature. Mid- and Near-IR electronic absorption spectra [22] suggested that the lowest lying excited electronic state of CoO located at 0.42 eV above the ground state, however this value was calculated to be 0.52 eV by Dolg et al. [31] and 0.36 eV with TD-B3LYP method in the prediction of Dai

et al. [32] Gutsev et al. [19] investigated the electronic state and geometrical structure of CoO$^-$ using DFT method and considered $^3\sum^-$ as the ground state for CoO$^-$, while Uzunova et al. [21] reported $^5\triangle$ to be the ground state. It is known that anion photoelectron spectroscopy is a reasonable approach for probing the electronic structure of clusters. Pramann et al. studied Co$_n$O$_m^-$ ($n$ = 4–20, $m$ = 0–2) using photoelectron spectroscopy [20] and suggested that their spectral features were contributed mainly from the Co 3d-derived orbitals and the oxygen atoms only had a minor influence on their electronic structures. So far, there is no photoelectron spectroscopy study on small Co$_n$O$^-$ ($n$ = 1–3) clusters. In this letter, we report the results obtained from the study on Co$_n$O$^-$ ($n$ = 1–3) cluster anions by photoelectron spectroscopy and density functional theory.

## 2. Experimental and computational methods

### 2.1. Experimental

The experiments were carried out using a home-built apparatus consisting of a time-of-flight (TOF) mass spectrometer and a magnetic-bottle photoelectron spectrometer, which was described elsewhere [33]. In brief, the Co$_n$O$^-$ ($n$ = 1–3) cluster anions were produced in a laser vaporization source composed of a rotating and translating cobalt target ablated with the second harmonic (532 nm) light pulses of a Nd:YAG laser, and helium gas with 4 atm. backing pressure was allowed to expand through a pulsed valve over the target. The residual oxygen in the carrier gas and on the target surface are enough for generating Co$_n$O$^-$ ($n$ = 1–3) clusters. The cluster anions were mass-analyzed by the TOF mass

spectrometer. The $Co_nO^-$ ($n$ = 1–3) clusters were each mass-selected and decelerated before being photodetached with the 532 or 266 nm laser beam from a second Nd:YAG laser. The electrons resulting from photodetachment were energy-analyzed by the magnetic-bottle photoelectron spectrometer. The photoelectron spectra were calibrated using the photoelectron spectrum of $Cu^-$ taken at similar conditions. The instrumental resolution was approximately 40 meV for electrons with 1 eV kinetic energy.

## 2.2. Computational methods

The theoretical calculations were performed using the BPW91 density-functional [34,35] with the 6-311 + G(d,p) basis set. The geometric structures of the anionic and the neutral species were determined by optimizing different initial geometries at several multiplicities. The optimizations were performed without imposing symmetry constraints and the calculated energies were corrected with the zero-point vibrational energies. Harmonic vibrational frequencies were calculated to make sure that the optimized structures correspond to real local minima. In addition, the term energy $\triangle E$ ($\tilde{A} \leftarrow \tilde{X}$) of the first excited state of CoO neutral was calculated with TD-DFT [36,37] and SAC-CI [38–40] methods. All the calculations were conducted with the Gaussian09 program package [41].

## 3. Results and discussion

The photoelectron spectra of $Co_nO^-$ ($n$ = 1–3) taken with 532 and 266 nm photons are shown in Figure 1. The photoelectron spectra taken with 532 nm photons show better resolution, whereas those with 266 nm photons provide the information

**Table 1**
Relative energies, VDEs and ADEs of the low energy isomers of $Co_nO^-$ ($n$ = 1–3) calculated at the BPW91 level of theory as well as the comparison with the experimental VDEs and ADEs.

| Isomer | | $\Delta E$ (eV) | ADE (eV) | | VDE (eV) | |
|---|---|---|---|---|---|---|
| | | | Theo. | Exp. | Theo. | Exp. |
| $CoO^-$ | 1A ($^3\sum^-$) | 0.00 | 1.35 | 1.54 ± 0.04 | 1.36 | 1.54 ± 0.04 |
| | 1B ($^5\sum$) | 0.003 | 1.35 | – | 1.39 | – |
| $Co_2O^-$ | 2A ($^6A'$) | 0.00 | 1.18 | – | 2.53 | – |
| | 2B ($^6B_2$) | 0.02 | 1.17 | 1.31 ± 0.08 | 1.19 | 1.43 ± 0.08 |
| | 2C ($^4A_1$) | 0.30 | 0.97 | – | 1.02 | – |
| | 2D ($^2A'$) | 0.31 | 1.40 | – | 1.65 | – |
| $Co_3O^-$ | 3A ($^9A$) | 0.00 | 1.32 | 1.38 ± 0.08 | 1.35 | 1.42 ± 0.08 |
| | 3B ($^7A$) | 0.20 | 1.13 | – | 1.76 | – |
| | 3C ($^7A$) | 0.46 | 1.04 | – | 1.13 | – |

concerning with the higher excited states of the neutral clusters. The adiabatic detachment energies (ADEs) and vertical detachment energies (VDEs) measured from the photoelectron spectra are listed in Table 1. The measurements of ADEs and VDEs by experimental photoelectron spectra were performed with the following methods. For VDE, the highest point of the first photoelectron peak profile was taken, and for ADE the measurement was completed by adding the value of the instrumental resolution to the onset of the first photoelectron peak profile. The optimized geometries of the typical low-lying isomers of $Co_nO^-$ and $Co_nO$ ($n$ = 1–3) are presented in Figure 3 with the most stable structures on the left. The calculated ADEs and VDEs are summarized in Table 1 along with the experimental VDEs and ADEs.
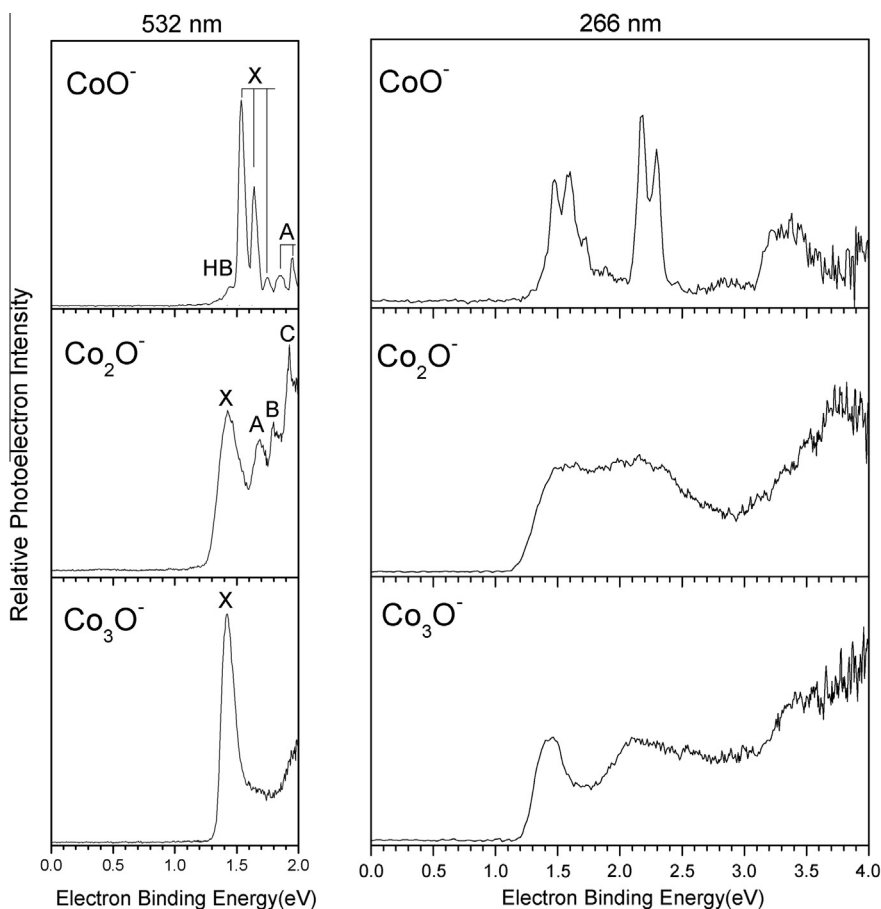


**Figure 1.** Photoelectron spectra of $Co_nO^-$ ($n$ = 1–3) taken with 532 and 266 nm photons. HB stands for hot bands.

## 3.1. Photoelectron spectra

$CoO^-$: The photoelectron spectrum of $CoO^-$ taken with 266 nm photons has been reported in our previous work [42]. It shows three major features in the range of 1.4–2.0, 2.1–2.5, and 3.1–4.0 eV, respectively. In order to see more details of the low electron binding features, we also measured the spectrum of $CoO^-$ with 532 nm photons. In the spectrum at 532 nm, the first major feature in the range of 1.4–2.0 eV is resolved into five sharp peaks centered at 1.54, 1.64, 1.74, 1.85, 1.95 eV, and a small shoulder at 1.45 eV. The small shoulder at 1.45 eV is a hot band, whereas the five sharp peaks can be tentatively assigned to the vibrational progressions related to the transitions from the ground state of $CoO^-$ to the electronic ground and excited states of CoO neutral. The first vibrational progression at lower electron binding energy is much intense, in which the vibrational spacing is about 0.10 eV ($806 cm^{-1}$), representing the transitions to the electronic ground state of CoO neutral. The second vibrational progression located at higher binding energy is tentatively identified as the transitions to the first electronic excited state of CoO neutral.

$Co_2O^-$: The photoelectron spectrum of $Co_2O^-$ at 266 nm has two broad features in the range of 1.40–2.54 and 3.53–4.00 eV. With 532 nm photons, four peaks centered at 1.43, 1.69, 1.80 and 1.92 eV are resolved for the low electron binding energy (EBE) part of the first broad feature.

$Co_3O^-$: The photoelectron spectrum of $Co_3O^-$ at 266 nm has a resolved peak centered at 1.42 eV, and two unresolved broad bands in the range of 2.02–2.53 and 3.40–4.00 eV. In the spectrum taken with 532 nm photons, the peak at 1.42 eV becomes sharper due to better resolution at 532 nm.

## 3.2. Theoretical calculations

$CoO^-$ and $CoO$: For $CoO^-$, we found that the $^3\sum^-$ (1A) and $^5\sum$ (1B) states are nearly degenerate, with $^5\sum$ higher than $^3\sum^-$ by only 0.003 eV in energy. The theoretical VDEs of $^3\sum^-$ (1A) and $^5\sum$ (1B) are both in agreement with the experimental measurement. Therefore, it is suggested that both isomers 1A and 1B contribute to the experimental photoelectron spectrum. The previous theoretical calculation conducted by Gutsev et al. [19] suggested $^3\sum^-$ as the ground state for $CoO^-$, while Uzunova et al. [21] reported $^5\triangle$ to be the ground state. Our calculations are consistent with the former. For isomer 1A, the calculated Co–O bond length is 1.62 Å, and the Wiberg bond order analysis using the NBO 3.1 program [43] shows that the Co–O bond order is 1.36, indicating that the Co–O bond is between typical single and double bond. For CoO neutral, our calculations show that the Co–O bond length of isomer 1A' (1.64 Å) is increased by 0.02 Å compared with that of the anion. The calculated vibrational frequency for CoO is about $816 cm^{-1}$ after a scale factor of 0.96, [44] consistent with the vibrational spacing observed in the experimental measurement.

In order to verify the assignment of the vibrational progressions, Franck–Condon factors simulations were performed to pinpoint the $0 \leftarrow 0$ band of $CoO(\tilde{X}) \leftarrow CoO^-(\tilde{X})$. The Franck–Condon factor simulations were conducted using the program developed by Liang et al. [45] In the spectrum simulation, a FWHM of $450 cm^{-1}$ was utilized with GAUSSIAN band envelopes. The simulated spectra of $CoO^-$ obtained by setting the temperature of anion at 550 and 0 K are presented in Figure 2 along with the experimental photoelectron spectrum. We can see that the simulated spectrum at 550 K (Figure 2b) is in excellent agreement with the experimental spectrum (Figure 2a), whereas, in the simulated spectrum at 0 K (Figure 2c), the 'hot band' at 1.45 eV is absent. Therefore, the simulation reveals that the temperature of $CoO^-$ generated in our laser ablation source is about 550 K. The peak at 1.54 eV corresponding to $CoO(\tilde{X}, v'' = 0) \leftarrow CoO^-(\tilde{X}, v' = 0)$ transition and the electron affinity of CoO is determined to be

$1.54 \pm 0.04$ eV. The peak at 1.85 eV is assigned as $0 \leftarrow 0$ band of $CoO(\tilde{A}) \leftarrow CoO^-(\tilde{X})$ transition and the term energy is evaluated to be 0.31 eV. The calculations of the term energy $\triangle E$ $(CoO(\tilde{A}) \leftarrow CoO(\tilde{X}))$ were conducted with TD-BPW91 and SAC-CI methods. The results are summarized in Table 2. At SAC-CI level, the calculated term energy is ~0.32 eV, in excellent agreement with the experimental value of 0.31 eV. The calculated value is ~0.25 eV with TD-BPW91 method, closing to the experimental value. Dai et al. [32] calculated the excited states of CoO using TD-B3LYP method, and they concluded that the first excited state of CoO was 0.36 eV higher than the ground state. Their value shows a good estimate compared with our experimental data. Danset et al. reported the lowest lying excited state is 0.42 eV above the ground state using Mid- and Near-IR electronic absorption spectrum, but this value was reduced to be 0.35 eV after two corrections [22]. Our result is close to the corrected value. It is worth mentioning that the electronic structures of $CoO^-$ and CoO have been studied in detail by Sakellaris et al. employing variational multireference configuration interaction (MRCI) and single-reference coupled-cluster methods [46].

$Co_2O^-$ and $Co_2O$: Four low-lying isomers for $Co_2O^-$ are given in Figure 3a. Isomer 2A has $C_s$ symmetry and is a quasi-linear structure in $^6A'$ electronic state. Isomer 2B is a $C_{2v}$ symmetry triangular structure in $^6B_2$ state, and the bond length of Co–O is 1.79 Å and that of Co–Co is 2.22 Å. Isomers 2A and 2B are nearly degenerate in energy with isomer 2B higher than isomer 2A by only 0.02 eV. The calculated VDE (1.19 eV) of the isomer 2B is close to the experimental VDE of 1.43 eV, and the theoretical ADE (1.17 eV) of 2B is also close to the experimental value of 1.31 eV. So we suggest that isomer 2B may exist in our experiment. The calculated VDE of isomer 2A is ~2.53 eV, much higher than the low EBE peaks in the experimental spectrum of $Co_2O^-$. It is possible that isomer 2A contributes to the high EBE features observed in the spectrum of $Co_2$-
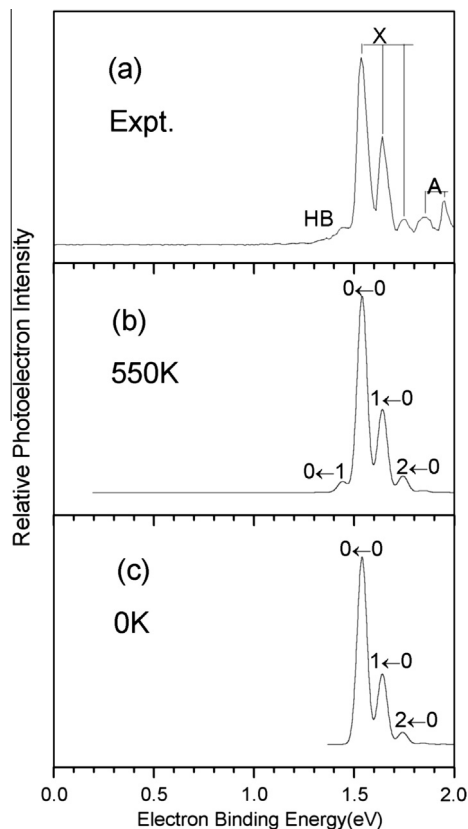


**Figure 2.** (a) Experimental photoelectron spectrum of $CoO^-$ taken with 532 nm photons. (b) Franck–Condon factor simulation at 550 K. (c) Franck–Condon factor simulation at 0 K.
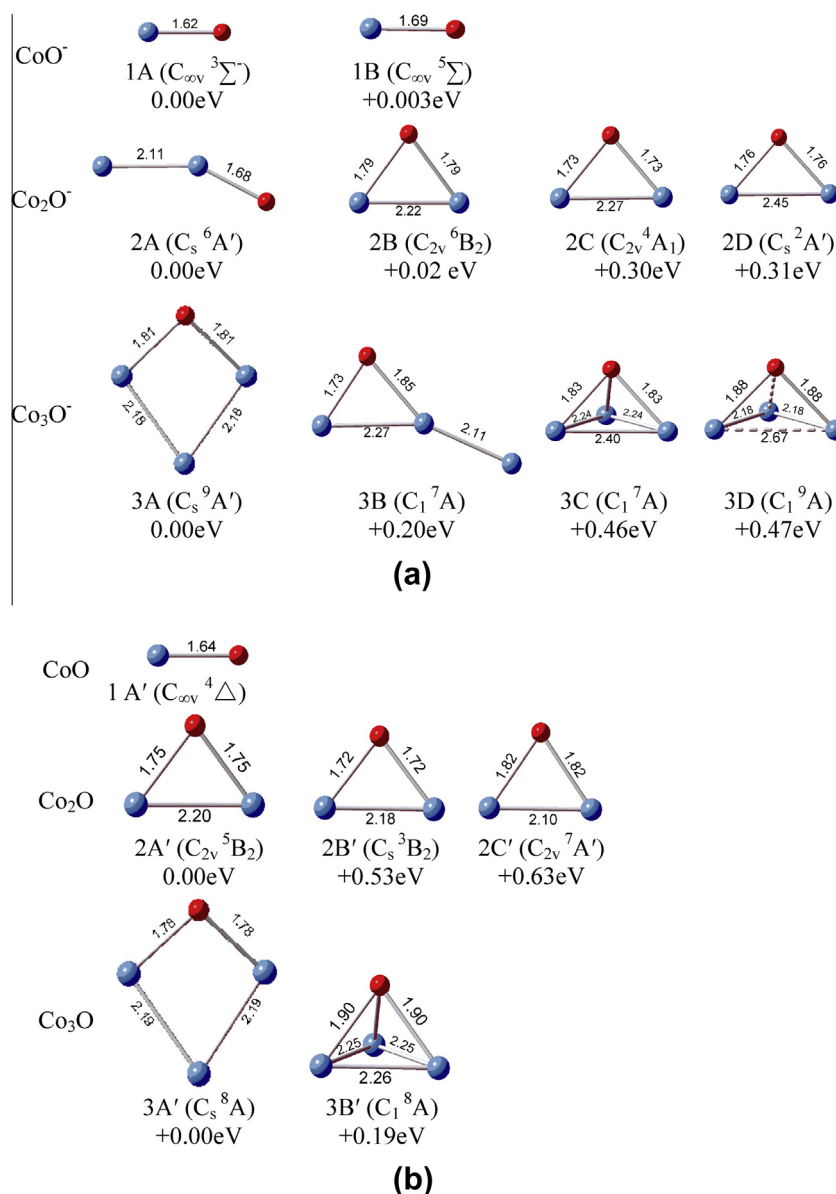
**Figure 3.** Optimized geometries of the low-lying isomers of (a) $Co_nO^-$ ($n$ = 1–3) and (b) $Co_nO$ ($n$ = 1–3) clusters. The bond lengths are in angstroms.

$O^-$. That can explain why the spectral features of the 266 nm spectrum of $Co_2O^-$ are so broad. For the other isomers, 2C and 2D are higher than isomer 2A by 0.30 and 0.31 eV respectively, thus, we consider that isomers 2C and 2D cannot make contribution to the experimental photoelectron spectrum of $Co_2O^-$. For the neutral $Co_2O$, the most stable isomer 2A′ is a triangular structure with $C_{2v}$ symmetry in $^5B_2$ state. Its Co-O bond length is 1.75 Å and Co–Co bond length is 2.20 Å. The isomers 2B′ in $^3B_2$ state and 2C′ in $^7A′$ state are 0.53 and 0.63 eV higher than isomer 2A′ in energy, respectively.

$Co_3O^-$ and $Co_3O$: The most stable structure of $Co_3O^-$, isomer 3A, is found to be a four-membered-ring with $C_s$ symmetry and in $^9A′$ electronic state, in which the oxygen is twofold coordinated. The bond lengths of Co-O and Co–Co are 1.81 and 2.18 Å, respectively. The calculated VDE (1.35 eV) and ADE (1.32 eV) of isomer 3A agree well with the experimental values. We suggest isomer 3A to be the one contributing to the experimental photoelectron spectrum of $Co_3O^-$. The EA of $Co_3O$ calculated by Liu et al. is about 1.42 eV [25], and our result is consistent with their value. Isomer 3B has a planar structure with the O atom attached to one of the Co atoms in $Co_3$ triangle. Its energy is higher than that of isomer 3A by

0.20 eV. The theoretical VDE of isomer 3B is calculated to be 1.76 eV, much higher than the experimental VDE 1.42 eV. So it could be excluded in our experiments. Isomers 3C and 3D are much higher than isomer 3A in energy. We therefore suggest that isomers 3C and 3D could not exist in our experiments. For the neutral $Co_3O$, isomer 3A′ (Figure 3b) has $C_s$ symmetry in $^8A$ state. Isomer 3B′ ($^8A$) is higher than 3A′ by 0.19 eV in energy.

### 3.3. Mulliken charges and magnetic properties

We carried out Mulliken population analysis to investigate the charges and magnetic moments on the Co and O atoms. The

**Table 2**
Calculated term energy of CoO as well as the comparison with the experimental value.

| Cluster | Term energy (eV) | | |
|---|---|---|---|
| | TD-DFT | SAC-CI | Experiment |
| CoO ($\tilde{A} \leftarrow \tilde{X}$) | 0.25 | 0.32 | 0.31 ± 0.04 |

**Table 3**
Mulliken charges, atomic magnetic moments ($\mu_A$), and total magnetic moments ($\mu_T$) of the most stable structures of $Co_nO^-$ ($n = 1$–3).

| Cluster | Atom | Mulliken charges (e) | $\mu_A$ ($\mu_B$) | $\mu_T$ ($\mu_B$) |
|---------|------|----------------------|-------------------|-------------------|
| $CoO^-$ | $Co_1$ | −0.33 | 1.49 | 2 |
| | $O_2$ | −0.67 | 0.51 | |
| $Co_2O^-$ | $Co_1$ | −0.25 | 2.29 | 5 |
| | $O_2$ | −0.49 | 0.41 | |
| | $Co_3$ | −0.25 | 2.29 | |
| $Co_3O^-$ | $Co_1$ | −0.16 | 2.59 | 8 |
| | $O_2$ | −0.49 | 0.50 | |
| | $Co_3$ | −0.16 | 2.59 | |
| | $Co_4$ | −0.19 | 2.32 | |

**Table 4**
Mulliken charges, atomic magnetic moments ($\mu_A$), and total magnetic moments ($\mu_T$) of the most stable structures of $Co_nO$ ($n = 1$–3).

| Cluster | Atom | Mulliken charges (e) | $\mu_A$ ($\mu_B$) | $\mu_T$ ($\mu_B$) |
|---------|------|----------------------|-------------------|-------------------|
| $CoO$ | $Co_1$ | 0.33 | 2.15 | 3 |
| | $O_2$ | −0.33 | 0.85 | |
| $Co_2O$ | $Co_1$ | 0.175 | 1.85 | 4 |
| | $O_2$ | −0.35 | 0.30 | |
| | $Co_3$ | 0.175 | 1.85 | |
| $Co_3O$ | $Co_1$ | 0.16 | 2.59 | 7 |
| | $O_2$ | −0.37 | 0.50 | |
| | $Co_3$ | 0.16 | 2.59 | |
| | $Co_4$ | 0.05 | 2.32 | |

charges and magnetic moments (spin densities) of $Co_nO^-$ ($n = 1$–3) and their corresponding neutrals are presented in Tables 3 and 4, respectively. As can be seen, the negative charges on the cobalt atoms of $Co_nO^-$ ($n = 1$–3) are 0.66e–0.88e higher than those of neutral $Co_nO$ ($n = 1$–3). Thus, we can see that the excess electrons are mainly localized at $Co_n$ sites. As for the magnetic moments, the calculated values for $Co_nO$ ($n = 1$–3) are 3, 4, 7 and for $Co_nO^-$ ($n = 1$–3) are 2, 5, 8 respectively. With the exception of $CoO^-$, the magnetic moments of the $Co_nO^-$ are higher than those of the corresponding neutrals by one. Additionally, in order to further understand the bonding models in these clusters, the electron densities of the molecular orbitals in $Co_nO^-$ ($n = 1$–3) are examined. The valence molecular orbitals of the lowest-energy configurations of $Co_nO^-$ ($n = 1$–3) are presented in Figure 4. We find that the highest occupied molecular orbitals (HOMOs) of these clusters are mainly localized over $Co_n$, which is consistent with their spin density distributions. The results imply that spectral features of $Co_nO^-$ ($n = 1$–3) were mainly contributed by Co 3d orbitals and the oxygen atoms had only minor influence on their electronic structures, which is consistent with the photoelectron spectroscopy study of the larger $Co_nO_m^-$ ($n = 4$–20, $m = 0$–2) clusters by Pramann et al. [20].

## 4. Conclusions

$Co_nO^-$ ($n = 1$–3) cluster anions were studied by a combined photoelectron experiment and density functional theory. The VDEs of $Co_nO^-$ ($n = 1$–3) were determined to be 1.54 ± 0.04, 1.43 ± 0.08, and 1.42 ± 0.08 eV respectively based on their photoelectron spectra. From vibrationally resolved photoelectron spectrum of $CoO^-$, we estimated that the electron affinity energy of $CoO$ is 1.54 ± 0.04 eV, and the term energy of the first excited state of $CoO$ is 0.31 ± 0.04 eV. The structures of these clusters and their corresponding neutrals were tentatively determined by comparing the calculated VDEs and ADEs with experimental values. The structure of $Co_2O^-$ is proposed to be triangular. $Co_3O^-$ is a quadrangle structure, and has a twofold coordinated oxygen atom. The
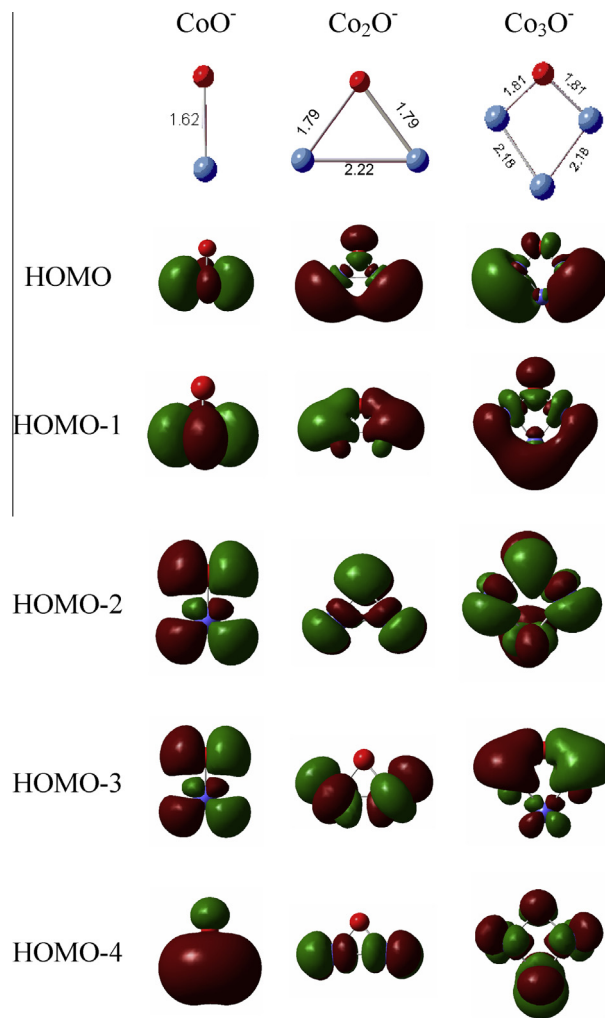


**Figure 4.** Diagrams of the molecule orbitals of $Co_nO^-$ ($n = 1$–3).

analysis of valence molecular orbitals shows that the distribution of electron densities of the HOMOs of the most stable isomers of $Co_nO^-$ ($n = 1$–3) mainly localizes over Co atoms.

## References

[1] C. Lin, J.A. Ritter, B.N. Popov, J. Electrochem. Soc. 145 (1998) 4097.
[2] G. Wang, Y. Chen, K. Konstantinov, M. Lindsay, H. Liu, S. Dou, J. Power Sources 109 (2002) 142.
[3] Y. Mergler, J. Hoebink, B. Nieuwenhuys, J. Catal. 167 (1997) 305.
[4] D. Pietrogiacomi, S. Tuti, M.C. Campa, V. Indovina, Appl. Catal. B 28 (2000) 43.
[5] J. Jansson, A.E.C. Palmqvist, E. Fridell, M. Skoglundh, L. Österlund, P. Thormählen, V. Langer, J. Catal. 211 (2002) 387.
[6] H.K. Lin, H.C. Chiu, H.C. Tsai, S.H. Chien, C.B. Wang, Catal. Lett. 88 (2003) 169.
[7] J. Wöllenstein, M. Burgmair, G. Plescher, T. Sulima, J. Hildenbrand, H. Böttner, I. Eisele, Sens. Actuators B 93 (2003) 442.
[8] X. Xie, Y. Li, Z.Q. Liu, M. Haruta, W. Shen, Nature 458 (2009) 746.
[9] D.B. Jacobson, B.S. Freiser, J. Am. Chem. Soc. 108 (1986) 27.
[10] R.B. Freas, B.I. Dunlap, B.A. Waite, J.E. Campana, J. Chem. Phys. 86 (1987) 1276.

[11] B.C. Guo, K.P. Kerns, A.W. Castleman, J. Phys. Chem. 96 (1992) 6931.
[12] R.J. Van Zee, Y.M. Hamrick, S. Li, W. Weltner, J. Phys. Chem. 96 (1992) 7247.
[13] D.J. Clouthier, G. Huang, A.J. Merer, E.J. Friedman-Hill, J. Chem. Phys. 99 (1993) 6336.
[14] M. Andersson, J.L. Persson, A. Rosen, J. Phys. Chem. 100 (1996) 12222.
[15] G.V. Chertihin, A. Citra, L. Andrews, C.W. Bauschlicher, J. Phys. Chem. A 101 (1997) 8793.
[16] E. Kapiloff, K.M. Ervin, J. Phys. Chem. A 101 (1997) 8460.
[17] M.R. Castell, S.L. Dudarev, G.A.D. Briggs, A.P. Sutton, Phys. Rev. B 59 (1999) 7342.
[18] M.A. Langell, M.D. Anderson, G.A. Carson, L. Peng, S. Smith, Phys. Rev. B 59 (1999) 4791.
[19] G.L. Gutsev, B.K. Rao, P. Jena, J. Phys. Chem. A 104 (2000) 5374.
[20] A. Pramann, K. Koyasu, A. Nakajima, K. Kaya, J. Phys. Chem. A 106 (2002) 4891.
[21] E.L. Uzunova, G.S. Nikolov, H. Mikosch, J. Phys. Chem. A 106 (2002) 4104.
[22] D. Danset, L. Manceron, J. Phys. Chem. A 107 (2003) 11324.
[23] F. Liu, F.-X. Li, P.B. Armentrout, J. Chem. Phys. 123 (2005) 064304.
[24] C.-C. Wang, R.-N. Zhao, J.-G. Han, J. Chem. Phys. 124 (2006) 194301.
[25] L. Liu, R.N. Zhao, J.G. Han, F.Y. Liu, G.Q. Pan, L.S. Sheng, J. Phys. Chem. A 113 (2009) 360.
[26] Y. Xie, F. Dong, S. Heinbuch, J.J. Rocca, E.R. Bernstein, Phys. Chem. Chem. Phys. 12 (2010) 947.
[27] S. Yin, W. Xue, X.-L. Ding, W.-G. Wang, S.-G. He, M.-F. Ge, Int. J. Mass Spectrom. 281 (2009) 72.
[28] C.J. Dibble, S.T. Akin, S. Ard, C.P. Fowler, M.A. Duncan, J. Phys. Chem. A 116 (2012) 5398.
[29] E.L. Uzunova, J. Phys. Chem. A 115 (2011) 10665.
[30] E.L. Uzunova, G.S. Nikolov, H. Mikosch, ChemPhysChem 5 (2004) 192.
[31] M. Dolg, U. Wedig, H. Stoll, H. Preuss, J. Chem. Phys. 86 (1987) 2123.
[32] B. Dai, K. Deng, J. Yang, Q. Zhu, J. Chem. Phys. 118 (2003) 9608.
[33] H.-G. Xu, Z.-G. Zhang, Y. Feng, J.-Y. Yuan, Y.-C. Zhao, W.-J. Zheng, Chem. Phys. Lett. 487 (2010) 204.
[34] A.D. Becke, Phys. Rev. A 38 (1988) 3098.
[35] J.P. Perdew, Y. Wang, Phys. Rev. B 45 (1992) 13244.
[36] R.E. Stratmann, G.E. Scuseria, M.J. Frisch, J. Chem. Phys. 109 (1998) 8218.
[37] M.E. Casida, C. Jamorski, K.C. Casida, D.R. Salahub, J. Chem. Phys. 108 (1998) 4439.
[38] H. Nakatsuji, K. Hirao, J. Chem. Phys. 68 (1978) 2053.
[39] J. Hasegawa, M. Ehara, H. Nakatsuji, Chem. Phys. 230 (1998) 23.
[40] T. Nakajima, H. Nakatsuji, Chem. Phys. 242 (1999) 177.
[41] M.J. Frisch et al., GAUSSIAN 09, Gaussian, Inc., Wallingford, CT, 2009.
[42] R.-Z. Li, H.-G. Xu, G.-J. Cao, Y.-C. Zhao, W.-J. Zheng, J. Chem. Phys. 135 (2011) 134307.
[43] E. D. Glendening, A. E. Reed, J. E. Carpenter, F. Weinhold., NBO Version 3.1.
[44] M.W. Wong, Chem. Phys. Lett. 256 (1996) 391.
[45] J. Liang, H. Li, J. Electron Spectrosc. Relat. Phenom. 135 (2004) 119.
[46] C.N. Sakellaris, A. Mavridis, J. Phys. Chem. A 116 (2012) 6935.